International Journal of Cosmetic Science

International Journal of Cosmetic Science, 2013, **35**, 272–280 doi: 10.1111/ics.12039

Singlet molecular oxygen quenching by the antioxidant dimethylmethoxy chromanol in solution and in *ex vivo* porcine skin

S. Nonell*, M. García-Díaz*, J. L. Viladot†, and R. Delgado†

*IQS School of Engineering, Molecular Engineering Group, Universitat Ramon Llull, Via Augusta 390, 08017, Barcelona, Spain and †Lipotec, S.A., Isaac Peral 17 (Polígon Industrial CamíRal), Gavà (Barcelona), Spain

Received 08 June 2012, Accepted 16 January 2013

Keywords: antioxidant, dimethylmethoxy chromanol, free radical, quenching, singlet oxygen

Synopsis

Singlet-oxygen is a non-radical reactive oxygen species believed to play a major role in many photooxidation processes in connection with diverse photo-biological processes such as skin ageing or photocarcinogenesis. Dimethylmethoxy chromanol (3,4-dihydro-6-hydroxy-2,2-dimethyl-7-methoxy-1(2H)-benzopyran) is a potent antioxidant used in cosmetic and pharmaceutical formulations. We have assessed the singlet oxygen quenching ability of dimethylmethoxy chromanol, by monitoring the near-IR phosphorescence of singlet-oxygen in solution and in *ex vivo* porcine skin samples. Dimethylmethoxy chromanol quenches singlet oxygen with a rate constant of $(1.3 \pm 0.1) \times 10^8\ M^{-1}\ s^{-1}$ in solution. Consistent with this, a clear reduction in the singlet oxygen lifetime and emission intensity was observed when *ex vivo* porcine skin samples were treated with dimethylmethoxy chromanol.

Résumé

L'oxygène singulet est une espèce non-radicalaires réactive de l'oxygène réputée jouer un rôle majeur dans des nombreux processus de photo-oxydation dans le cadre de divers processus photo-biologiques comme le vieillissement de la peau ou la photocarcinogénèse. Le Dimethylmethoxy chromanol (3,4-dihydro-6-hydroxy-2,2-diméthyl-7-méthoxy-1 (2H)-benzopyran) est un antioxydant puissant utilisé dans des formulations pharmaceutiques et cosmétique. Nous avons évalué la capacité de quenching de l'oxygène singulet par le chromanol dimethylmethoxy, en suivant la phosphorescence dans l'infrarouge proche de l'oxygène singulet en solution et dans des échantillons de peau de porc *ex-vivo*. Le Dimethylmethoxy-chromanol épuise l'oxygène singulet avec une vitesse constante de $(1{,}3 \pm 0{,}1) \times 10^8 M^{-1}s^{-1}$en solution. Conformément à cela, une nette diminution de la durée de vie et de l'intensité des émissions de l'oxygène singulet a été observée lorsque des échantillons de peau de porc *ex-vivo* ont été traités avec le chromanol dimethylmethoxy.

Correspondence: Josep-Lluís Viladot, Lipotec, S.A., Isaac Peral 17 (Polígon Industrial CamíRal), Gavà (Barcelona), Spain. Tel: +34 936 388 000. Fax: +34 936 388 093. e-mail: jviladot@lipotec.com; Santi Nonell, Grup d'Enginyeria Molecular, IQS School of Engineering, Universitat Ramon Llull, Via Augusta 390, 08017 Barcelona, Spain. Tel: +34 932 672 000. Fax: +34 932 056 266. e-mail: santi.nonell@iqs.url.edu

Introduction

The inclusion of antioxidants in cosmetic preparations is an increasing trend [1, 2]. This is based on the rationale that skin is chronically exposed to radicals and other oxidising species whose damaging potential can be minimized by appropriate scavengers [3]. Although commonly used, the term antioxidant is nevertheless rather vague, referring generically to the ability of scavenging free radicals and other oxidising species such as (i) reactive oxygen species (ROS), e.g., hydroxyl radicals ($HO^{\bullet}$), superoxide anion (O_2^{-}), hydrogen peroxide (H_2O_2), and singlet molecular oxygen [$O_2(a^1\Delta_g)$ or $^1O_2$], (ii) reactive carbonyl species (RCS), carbonyl intermediates originated from lipid peroxidation and glycation, such as 4-hydroxy-2-nonenal, acrolein, malondialdehyde and glyoxal, (iii) reactive nitrogen species (RNS), i.e., radical-nitrogen based molecules that can act to facilitate nitrosylation reactions [4].

These species are beneficially involved in many signalling pathways and a regulated redox balance exists with endogenous antioxidant molecules that protects cells from the injurious attack of ROS and their counterparts [5] (Fig. 1). Biological defence against ROS comprises a complex array of antioxidants, enzymes, endogenous antioxidant factors such as haem proteins, coenzyme Q and bilirubin, and a variety of nutritional factors, primarily antioxidant vitamins [6, 7]. The significance of ROS species in connection with diverse biological processes such as skin ageing, inflammation, carcinogenesis, degenerative neurological diseases or radiation damage has prompted, especially in recent years, a boost on antioxidant research.

Due to its interface function between the body and environment, skin is chronically exposed to both endogenous and environmental pro-oxidant agents. These free radicals are generated from endogenous sources, such as enzyme activity or activated neutrophils, and also external pro-oxidant stimuli, such as ultraviolet radiation.

In contrast to UVB that leads to direct sunburn and DNA damage, UVA radiation mainly triggers photosensitized reactions by exciting endogenous and exogenous photosensitisers (PSs). Subsequently produced ROS, damage DNA bases related with photocarcinogenesis [8], accelerate collagen breakdown and decrease collagen synthesis responsible for skin ageing [9], and promote the expression of pro-inflammatory genes relevant to the pathogenesis of photodermatosis [10]. A large number of endogenous PSs have been identified, e.g., flavins, porphyrins, NADH/NAD or urocanic acid [11–14]. Exogenous molecules, frequently administered to skin along with cosmetic or medical treatments, also produce ROS

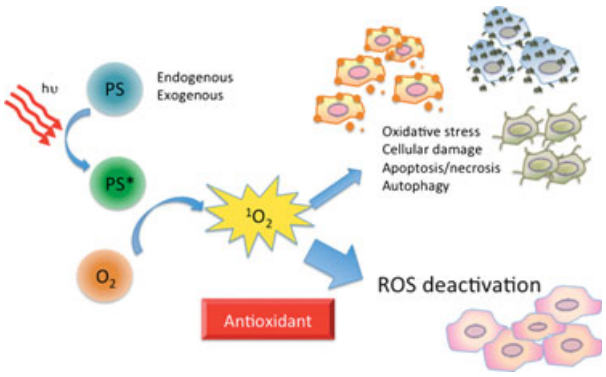

Figure 1 Mechanism of ROS deactivation by antioxidants. Singlet oxygen is generated by energy transfer from the triplet excited state of the photosensitiser. This highly cytotoxic agent together with the rest of ROS, induces oxidative stress leading to apoptosis, necrosis or autophagy. The action of antioxidants is to provide protection against cellular damage by deactivating ROS production.

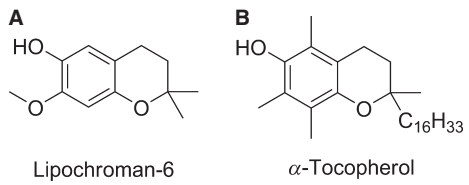

Figure 2 Chemical structures of (A) LC-6 and (B) α-tocopherol.

under UVA exposure. Antibiotics [15, 16], some non-steroidal anti-inflammatory drugs and antidepressants [17, 18] or other exogenous compounds [19] are a source of light-driven ROS formation.

Dimethylmethoxy chromanol (3,4-Dihydro-6-hydroxy-2,2-dimethyl-7-methoxy-1(*2H*)-benzopyran, CAS number 83923-51-7; LC-6, Fig. 2) is a powerful antioxidant used in cosmetic and pharmaceutical formulations. Its antioxidant activity has been evaluated as a part of a study for an interlaboratory comparison to assess the antioxidant potentials of several compounds [20]. LC-6 yielded the best results with the 2-thiobarbituric acid (TBA) assay based on the prevention of the formation of malondialdehyde, a degradation product of lipid peroxidation. The other tested compounds were a series of common antioxidants such as 3,5-di-tert-butyl-4-hydroxytoluene (BHT), trolox, tocopherol and 4-methylbrenzcatechin. Besides the TBA assay, one *in vivo* and several *in vitro* antioxidant assays describe the efficient ROS and RNS scavenging ability of LC-6, as summarized in Table I.

As the structure of LC-6 resembles that of α-tocopherol (Fig. 2), a common antioxidant that has also been described as an effective singlet oxygen (hereafter $^1O_2$) quencher [27] and that $^1O_2$ is indeed produced upon exposure of skin to UVA [12, 28], it seems plausible that the LC-6 antioxidant activity may be, at least partially, due to quenching of $^1O_2$.

'Singlet oxygen' is the term coined to refer to the dioxygen molecule in its singlet electronic excited state. It is a non-radical ROS that, due to the relative ease by which it is generated in the presence of light, it is believed to play a major role in many photooxidation processes, reacting rapidly with electron-rich substances such as unsaturated hydrocarbons, phenols, amines or sulphides, commonly located in membrane lipids, as well as with proteins and DNA [29–31]. Production of $^1O_2$ by photochemical pathways is rather straightforward: absorption of light energy by a suitable molecule referred to as the photosensitiser (PS) results in the population of its excited states (PS*), from which energy transfer to nearby oxygen molecules can occur, ultimately yielding $^1O_2$ as illustrated in Scheme 1:

$$\mathrm{PS} + h\nu \rightarrow {}^1\mathrm{PS}^*$$
$${}^1\mathrm{PS}^* \rightarrow {}^3\mathrm{PS}^*$$
$${}^3\mathrm{PS}^* + \mathrm{O}_2 \rightarrow \mathrm{PS} + {}^1\mathrm{O}_2$$

Scheme 1 Scheme 1. Mechanism of singlet oxygen photosensitization. Absorption of light by a photosensitiser PS, promotes it to its singlet electronic excited state (^{1}PS*). Radiationless processes change its spin from singlet to triplet (^{3}PS*), which then transfers its energy to ambient dioxygen molecules yielding $^1O_2$.

Once produced, $^1O_2$ may diffuse away from the site of production and oxidise susceptible substrates before it decays, a process that is complete within a few microseconds in biological media. A tiny (10^{-5}–10^{-7}) fraction of $^1O_2$ molecules undergoes radioactive decay emitting a photon in the near infrared. This extremely weak phosphorescence, centred at 1275 nm, provides the means for the most direct and unambiguous method for $^1O_2$ detection. The time-resolved measurement of this NIR emission is now a very well-established technique, for monitoring $^1O_2$ [32, 33]. The production and decay of $^1O_2$ in a pulsed photosensitization process obeys a bi-exponential kinetic model:

$$\left[{}^1\mathrm{O}_2\right]_t = \left[{}^1\mathrm{O}_2\right]_0 \cdot \frac{\tau_\Delta}{\tau_\Delta - \tau_T}\left(e^{-t/\tau_\Delta} - e^{-t/\tau_T}\right) \quad (1)$$

where τ_T is the lifetime of ^{3}PS* and τ_Δ is the lifetime of $^1O_2$, and $[^1O_2]_0$ is the concentration of $^1O_2$ produced by the laser pulse.

Thus, the goal of the work reported here is to characterize the $^1O_2$ quenching ability of LC-6 in solution and in an *ex vivo* porcine skin model.

Materials and methods

Chemicals

LC-6 (Lipochroman™) and Preventhelia™ were supplied by Lipotec S.A. LC-6 was certified to be of purity higher than 96%. Preventhelia™ is an aqueous solution of 0.05% diaminopropionyl tripeptide-33 (CAS number 1199495-15-2, MW 409,45 g·mol^{-1}, theoretical logP -4.66) preserved with 0.5% caprylyl glycol that acts as scavenger of RCS, thus inhibiting the carbonylation of proteins involved in DNA repair by 4-hydroxynonenal. It is formulated together with LC-6 to provide an integral protection against the diversity of different radical species. *d,l*-α-Tocopherol was purchased from BASF Aktiengesellschaft (Limburgerhof, Germany). Phenonip® was purchased from Clariant AG (Pratteln, Switzerland). 1*H*-phenalen-1-one (PN, 97%), 5,10,15,20-tetraphenyl-21*H*,23*H*-porphine (TPP, ≥ 99%), and 5,10,15,20-tetrakis (N-methyl-4-pyridyl)-21*H*,23*H*-porphine (TMPyP, 97%) were purchased from Sigma-Aldrich Chemical Co. (St. Louis, MO). Deuterium oxide (99.9%) and methanol-d_4 (99.8%) were purchased from Solvents Documentation Synthesis (SDS, Peypin, France). All other chemicals were commercially available reagents of at least analytical grade.

Table I Antioxidant activity tests reported for LC-6 (dimethylmethoxy chromanol)

Test	Measurement	Result for LC-6	Reference
1	*In vitro* inhibition of 3-nitrotyrosine formation by peroxynitrite.	LC-6 acted as a RNS scavenger preventing the nitration of tyrosine.	[4]
2	Glutamate neurotoxicity in cerebellar neurons mediated by excessive production of nitric oxide (NO).	LC-6 acted as a NO scavenger in neurons preventing glutamate neurotoxicity.	[21]
3	Indirect fluorometric screening test of total oxidative stress, based on the prevention of the formation of malodialdehyde (MA) from TBA.	Best result in a series comprising also BHT, Trolox, Tocopherol and 4-methylbrenzcatechin.	[20]
4	Analysis of inhibition of dichlorofluorescein oxidation in cell cultures.	Third position after Tocopherol and 4-methylbrenzcatechin in a series also comprising BHT, Trolox and ascorbic acid.	[20]
5	Inhibitory effect on rat liver microsomal lipid peroxidation enzymatically stimulated by NAPDH or chemically stimulated with Fe(II) and ascorbate.	LC-6 was a potent lipid peroxidation inhibitor.	[22,23]
6	Protection of glutathione peroxidase (GPx) against glucose-induced inactivation, *in vitro* and *in vivo*.	*In vitro*, LC-6 protected GPx activity from glucose-induced inactivation. *In vivo*, LC-6 administration prevented the alterations of oxidative stress markers (tissue glutathione and MDA concentration, and GPx activity) and the impairment of retinal function.	[24]
7	Oxidative stress-mediated apoptosis induced with H_2O_2 on a model cell system (human neuroblastoma cell line SH-SYSY).	LC-6 protected SH-SYSY neuroblastoma cells from oxidative stress-induced apoptosis.	[25]
8	Oxidative stress-induced apoptosis in retinal photoreceptor cells treated with the nitric oxide donor sodium nitroprusside.	Oxidative stress-induced apoptosis in retinal photoreceptor cells was mediated by calpains and caspases and blocked by LC-6.	[26]
9	Internal photoprotection capacity against UVA radiation assayed in primary cultures of human melanocytes using the alkaline comet assay to quantify DNA damage in individual eukaryotic cells.	Inhibition of DNA damage in a dose-dependent manner due to ROS production inhibition.	([a])
10	Fibroblast cell culture viability under oxidative stress by hydrogen peroxide.	LC-6 protected human fibroblasts against oxidative stress, being more active than resveratrol, tocopherol and ferulic acid.	([a])
11	Antioxidative power (AP) by monitoring of the reducing activity against the stable test cation radical diphenylpicryl-hydrazyl	Strong antioxidant capacity with AP values comprised between 1130000 and 1470000 AU and reaction times from 0.20 to 0.17 min.	([a])
12	Inhibition of peroxide formation in essential oils, by measurement of iodine formation.	Complete inhibition of peroxide formation after 2 weeks incubation of essential oils with 0.01% LC-6 at 60°C.	([a])

[a]Unpublished results, manuscript in preparation.

Cream preparations

LC-6 and α-tocopherol creams containing 3% of either PN or TPP were prepared with the compositions and procedure described in Table II.

Porcine skin

The skin used in this study was obtained from the back of pigs because of its similarity to human skin. Skin from female pigs of about 30 kg, used as negative controls for research and education purposes, was obtained from the Facultat de Veterinària of the Autonomous University of Barcelona. The skin was dermatomed to a thickness of about 500 μm. Skin discs were prepared with a diameter of 2.5 cm. Skin thickness was measured and the biopsies with values outside the range between 300 and 700 μm were discarded.

Furthermore, the integrity of the skin was evaluated by the transepidermal water loss (TEWL) measurement. A TEWL value of 5–10 $g/m^2 \cdot h$ is taken as an indication of healthy skin [34] and the value of 15 $g/m^2 \cdot h$ is commonly taken as an acceptable upper limit for skin permeability studies [35, 36]. Thus, only the biopsies with a TEWL value lower than 15 $g/m^2 \cdot h$ were used in the experiments.

Singlet oxygen measurements

$^1O_2$ phosphorescence was detected using a customized PicoQuant Fluotime 200 system (Fig 3.) described elsewhere [33]. A diode-pumped pulsed Nd:YAG laser (FTSS355-Q, Crystal Laser, Berlin, Germany) working at 10 kHz repetition rate and emitting 1 ns laser light-pulses either at 355 nm (5 mW, 0.5 μJ per pulse) or 532 nm (10 mW, 1 μJ per pulse) was used for excitation. A 1064 nm rugate notch filter (Edmund Optics, York, U.K.) was

Table II Composition of the LC-6 and α-tocopherol creams containing 3% of PN or TPP. Preparation procedure: 1) prepare mixture A at 70–75°C dispersing the photosensitizer (PN or TPP) in the lipid components, 2) prepare mixture B by stirring all B components at 65–70°C, with slow addition of Carbomer, 3) slowly add mixture A over mixture B with gentle stirring, 4) cool previous mixture to 40–50°C and add component C, 5) successively add components D and E while stirring. Final pH was comprised in the range 5.5–7.5

		Percentage composition (%)			
Phase	**Ingredients(*Inci Names in Italics*)**	**Placebo cream**	**Cream containing 0.1% α-tocopherol**	**Cream containing 0.01% LC-6**	**Cream containing 0.05% LC-6**
A	*Mineral oil (Paraffinum liquidum)*	10	10	10	10
A	*Stearic acid*	3	3	3	3
A	*Cetearyl alcohol*	2	2	2	2
A	*Beeswax (Cera Alba)*	1	1	1	1
A	*Tocopherol*	–	0.1	–	–
A	LC-6 (Lipochroman™, *Dimethylmethoxy chromanol*)	–	–	0.01	0.05
A	Photosensitizer (PN or TPP)	3	3	3	3
B	*Water (Aqua)*	78.4/73.4[a]	78.3	76.39	73.35
B	*Glycerin*	3	3	3	3
B	Phenonip® (*Phenoxyethanol, Methylparaben, Ethylparaben, Butylparaben, Propylparaben, Isobutylparaben)*	0.6	0.6	0.6	0.6
B	*Carbomer*	0.2	0.2	0.2	0.2
C	*Dimethicone*	0.2	0.2	0.2	0.2
D	*Triethanolamine*	0.6	0.6	0.6	0.6
E	Preventhelia™ (*Water (Aqua), Diaminopropionoyl Tripeptide-33, Caprylyl Glycol*)	/5[a]	–	2	5

[a]Placebo creams were prepared with and without Preventhelia™.

placed at the exit port of the laser to remove any residual component of its fundamental emission in the near-IR region. The size of the laser beam was adjusted to ca. 1 × 3 mm at the surface of the samples. The luminescence exiting from the cuvette or solid sample was collected by an f = 15 cm lens, passed through a cold mirror and a series of long-pass filters of increasing cut-off wavelengths (CVI Melles Griot, Albuquerque, NM) to remove any scattered laser irradiation, and filtered by suitable interference filters to isolate the $^1O_2$ emission. A TE-cooled Hamamatsu NIR photomultiplier (model H9170-45), sensitive from 950 to 1400 nm, was used to detect the conditioned NIR luminescence. The detector was operated in photon counting mode and its output sent to a PicoQuant NanoHarp 250 multichannel scaler working at 128 ns per channel. The count histograms were built up until a sufficient signal-to-noise ratio was attained. The kinetic model in Eq. 1 was fitted to the count histograms using the FluoFit 4.0 software, from which the kinetic rate constant governing $^1O_2$ formation and decay were calculated.

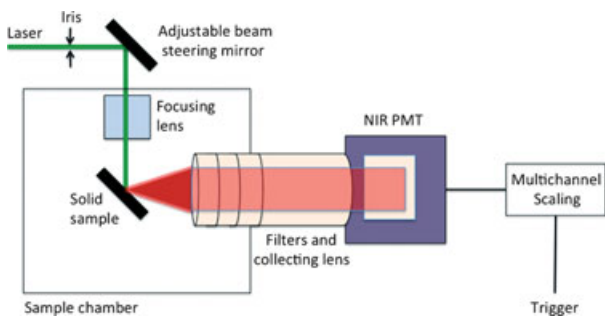

Figure 3 Experimental set-up for the photon counting time- and spectrally resolved singlet-oxygen phosphorescence detection.

LC-6 quenching of singlet oxygen in solution

The decay of $^1O_2$ is accelerated by added quenchers such as LC-6 (Scheme 2):

$$k_\Delta = \frac{1}{\tau_\Delta} = k_0 + k_{LC6}[LC6] \quad (2)$$

$$^1O_2 \xrightarrow{k_0} O_2$$

$$^1O_2 + LC6 \xrightarrow{k_{LC6}} \text{Products}$$

Scheme 2 Scheme 2. Pathways of $^1O_2$ decay in the absence or presence of LC-6. The rate constant of $^1O_2$ quenching by LC-6 (k_{LC6}) was thus determined by measuring its effect on the kinetics of $^1O_2$ decay [37]. According to Scheme 2, the observed rate constant for $^1O_2$ decay (k_Δ) should increase linearly with the concentration of LC-6 (Eq. 2).

where τ_Δ is the actual $^1O_2$ lifetime and k_0 is the decay rate constant in the absence of quencher. Thus, a plot of k_Δ vs. [LC6] was constructed by adding increasing amounts of LC-6 to a PS solution and recording the kinetics of $^1O_2$ production and decay. 1*H*-Phenalen-1-one (PN) 80 μM in methanol-d_4 (CD_3OD) was used

as PS [38–40]. The slope of the linear plot obtained yielded k_{LC6}. The result quoted corresponds to the average of three independent determinations.

LC-6 quenching of singlet oxygen in *ex vivo* porcine skin

15 mg (5 mg/cm^2) of LC-6 formulations containing 3% of PN or TPP were spread on porcine skin samples over the whole surface using a glove-coated finger. In a first series of experiments, $^1O_2$ measurements were carried out 15 min or 24 h later to allow for cream penetration in the skin using the irradiation conditions described above. In another series of experiments, the skin surface was thoroughly washed with a solution of sodium dodecyl sulphate after the incubation period of 24 h in order to remove any PS that had not penetrated into the skin. Finally, a series of experiments was carried out applying the water-soluble TMPyP, which has very recently been shown to accumulate in the stratum corneum of porcine skin [41]. Skin was incubated overnight with an aqueous solution of 500 μM TMPyP. $^1O_2$ measurements were performed before and after washing the treated skin. 0.1 mM LC-6 solution in DMSO was then applied to TMPyP treated skin and $^1O_2$ measurements were recorded again. In all cases, capturing a typical $^1O_2$ phosphorescence signal took approximately 20 s. Five measurements were recorded at different positions of the skin surface and averaged to compensate for sample in homogeneity. A placebo cream (without LC-6) and a α-tocopherol containing cream were used as negative and positive controls respectively. Untreated skin was used as blank. Experiments were repeated on at least three different skin samples and the data reported are the average between such measurements.

Results

LC-6 quenching of singlet oxygen in solution

The time-resolved $^1O_2$ phosphorescence curves for each LC-6 solution are collected in Fig. 4A. In the absence of LC-6, the lifetime of $^1O_2$ was 210 $\pm$ 20 μs, which agrees well with the published value of 240 $\pm$ 20 μs in CD_3OD [37]. Addition of LC-6 resulted in a clear decrease in the $^1O_2$ lifetime τ_Δ. From the plot of the decay rate constant k_Δ (=1/τ_Δ) as a function of LC-6 concentration, the value of the quenching rate constant $k_{LC6} = (1.3 \pm 0.1) \times 10^8$ M^{-1} s^{-1} was determined (Fig. 4).

LC-6 quenching of singlet oxygen in *ex vivo* porcine skin samples

A similar approach was followed to probe the effect of LC-6 on $^1O_2$ in *ex vivo* samples of porcine skin. Because skin is a heterogeneous medium, five time-resolved $^1O_2$ phosphorescence curves, recorded at different positions of skin, were averaged for each formulation tested. In the first series of experiments, formulations containing PN as PS were applied to the skin and after 15 min or 24 h of penetration, $^1O_2$ phosphorescence measurements were carried out. Figure 5 shows the 1275-nm time-resolved luminescence signals for the different formulations in skin. When placebo was applied to porcine skin, the decay time of $^1O_2$ luminescence grew with a lifetime of $\tau_1 = 0.8 \pm 0.3$ μs and decayed with a lifetime of $\tau_2 = 18 \pm 2$ μs (Fig. 5A) ir pective of the cream penetration time. The former was assigned to the formation of $^1O_2$ and thus to the decay of the triplet PN precursor (τ_T in Eq. 1), while the latter was assigned to $^1O_2$ decay (τ_Δ in Eq. 1). In addition, we tested an alternative placebo sample lacking the Preventhelia™additive and found the same rates for $^1O_2$ production and decay, which rules out any effect of this additive. On the other hand, LC-6 induced concentration-dependent significant changes to the $^1O_2$ kinetics (Figs. 5B and 5C). At LC-6 0.05% w/w and either 15 min or 24 h cream penetration time, the lifetime of $^1O_2$ dropped to $\tau_{\Delta1} = 5 \pm 2$ μs and an additional long-lived decay component could be observed with $\tau_{\Delta2} = 13 \pm 2$ μs (relative amplitude 1:2). For comparison, α-tocopherol at 0.1% w/w quenched both the formation and the decay of $^1O_2$, yielding a low intensity signal with lifetime $\tau_\Delta = 3 \pm 2$ μs, once again independent of the cream penetration time (Fig. 5D).

PN, as a partially water soluble molecule, can localize in both the lipid and aqueous compartments of the skin. However, the high lipophilicity of LC-6 suggests its preferential accumulation in hydrophobic domains. To ensure a closer proximity between the nascent $^1O_2$ and LC-6, a more hydrophobic PS, TPP [37], was used in another series of experiments. As with PN, the NIR emission spectra showed a maximum at 1275 nm, which is the unambiguous spectroscopic fingerprint of $^1O_2$ (Fig. 6). Consistent with the lifetime decrease observed with PN, the $^1O_2$ phosphorescence dropped by ca. 50% when LC-6 0.05% was added to the cream. Under the same conditions, α-tocopherol led to almost complete depletion of the $^1O_2$ emission.

A third series of experiments were carried out on skin samples that were thoroughly washed with a solution of sodium dodecyl sulphate after the incubation period of 24 h. The lifetime data for

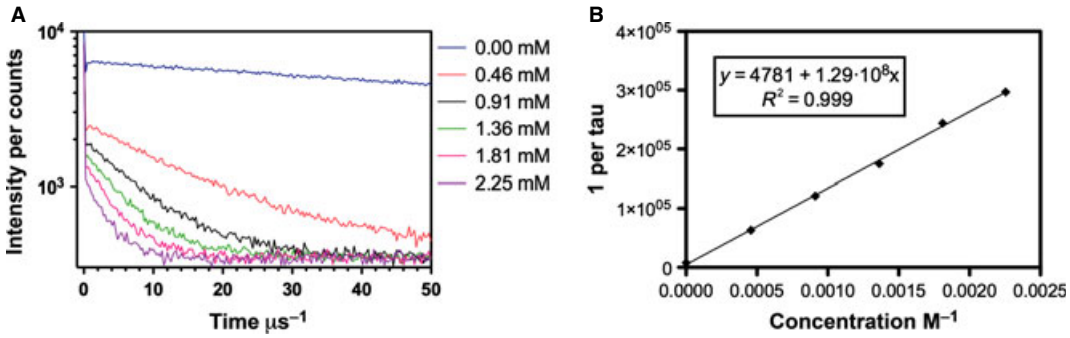

Figure 4 Effect of LC-6 on the kinetics of singlet-oxygen decay in methanol-d_4. (A) Time-resolved singlet-oxygen phosphorescence curves recorded at 1275 nm upon irradiation of PN solution containing different concentrations of LC-6 (B) Stern-Volmer plot of PN solution upon addition of increasing amounts of LC-6.

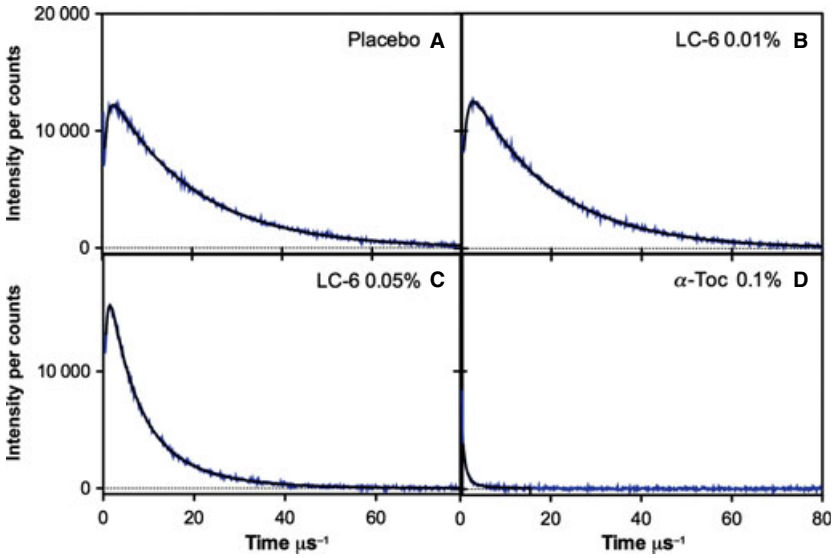

Figure 5 Time-resolved luminescence decays recorded on 355 nm excitation of *ex vivo* porcine skin treated with different PN containing formulations. (A) Placebo cream. Fitted parameters: $\tau_T = 0.8 \pm 0.3$ μs; $\tau_\Delta = 18 \pm 2$ μs. (B) LC-6 0.01% cream. Fitted parameters: $\tau_T = 0.9 \pm 0.3$ μs; $\tau_\Delta = 18 \pm 2$ μs. (C) LC-6 0.05% cream. Fitted parameters: $\tau_T = 0.8 \pm 0.2$ μs; $\tau_{\Delta 1} = 5 \pm 2$ μs; $\tau_{\Delta 2} = 13 \pm 2$ μs. (D) α-tocopherol cream. Fitted parameter: $\tau_\Delta = 3 \pm 2$ μs.

the placebo cream remained as in the previous experiments. However, in the presence of 0.05% LC-6 only the shortest of the two decay components observed previously could be detected, with a lifetime very similar to that observed in the presence of 0.1% α-tocopherol (5 ± 2 and 3 ± 2 μs respectively; Fig. 7).

Finally, an additional series of measurements were carried out applying TMPyP, which accumulates in the stratum corneum of pig skin [41]. Using this PS we obtained a single decay lifetime value of 18 ± 2 μs, with or without washing, that decreased to 8 ± 3 μs when 300 μL of a 0.1 mM LC-6 solution in DMSO were added (Fig. 8).

Discussion

A variety of methods exist for assessing the ability of an antioxidant to quench $^1O_2$. Techniques such as electron spin resonance (ESR) [42–45], lipid photooxidation [46–48], the oxygen radical absorbance capacity (ORAC) [49, 50] or its variation, the singlet oxygen absorption capacity (SOAC) assay methods [51, 52] are often used. However, these methods can lead to considerable errors as $^1O_2$ is not probed directly and unambiguously [53]. Moreover, their application *in vivo* is also limited as some of these probes are either toxic or do not penetrate tissue to a sufficient extent. In this work, we have monitored $^1O_2$ quenching by its time-resolved phosphorescence, which is regarded as the most specific means for reliable $^1O_2$ detection. At present, this work represents the first report of $^1O_2$ quenching activity of an antioxidant in skin.

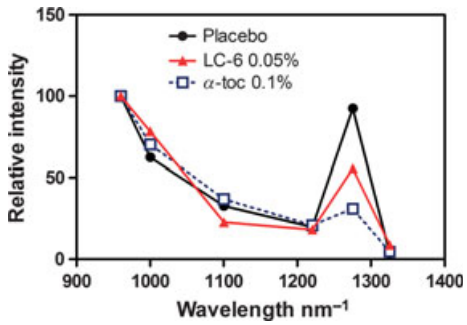

Figure 6 Spectra of singlet-oxygen luminescence at different wavelengths recorded on 532 nm excitation of *ex vivo* porcine skin treated with different TPP containing formulations.

Tocopherols rank among the most effective $^1O_2$ scavengers (Fig. 2B) and are broadly used in the cosmetic as well as in other sectors, e.g., food [54]. Thus, α-tocopherol quenches $^1O_2$ with a bimolecular rate constant that increases with the dielectric constant of the medium [55], e.g., 2.8×10^8 $M^{-1}s^{-1}$ in monodeuterated methanol [55]. This value is ca. two-fold the value found for LC-6. The reactivity of tocopherols towards $^1O_2$ correlates well with their biological activity and it has been suggested that one of the functions of vitamin E might be to protect membrane lipids form oxidative damage by $^1O_2$ [56].

To test whether this observation holds in skin, we formulated two concentrations of LC-6, namely 0.01% and 0.05%, and compared them with 0.1% α-tocopherol formulation. A placebo cream without antioxidants was used as negative control.

The luminescence of $^1O_2$ has been detected previously in *ex vivo* porcine skin and *in vivo,* human skin samples exposed to UVA radiation without any exogenous PS added [28]. However, the intensity of this signal was too small for the determination of quenching efficacy of antioxidants [57]. Thus, an external PS was added in our experiments to obtain phosphorescence signals with the necessary quality. Because the detection system is not able to discriminate between signals generated on or in the skin, we conducted two series of experiments in which the skin surface was or was not washed after PS application. The PN-photosensi-

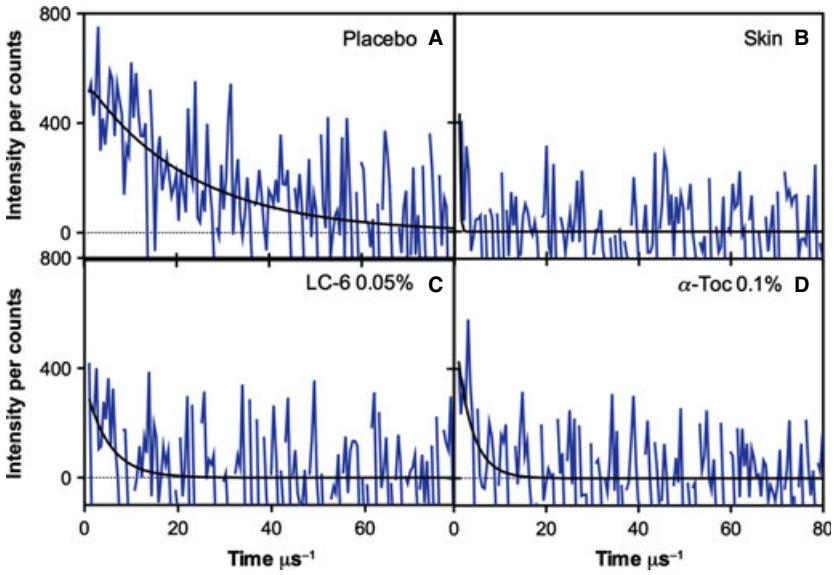

Figure 7 Time-resolved luminescence decays recorded on 355 nm excitation of *ex vivo* porcine skin treated with different PN containing formulations and thoroughly washed after incubation. (A) Placebo cream. Fitted parameters: $\tau_\Delta = 22 \pm 4$ μs. (B) Untreated skin. (C) LC-6 0.05% cream. Fitted parameters: $\tau_\Delta = 5 \pm 2$ μs. (D) α-tocopherol cream. Fitted parameter: $\tau_\Delta = 3 \pm 2$ μs.

tised generation of $^1O_2$ in the skin yielded a decay time of 18 ± 2 μs when the placebo cream was applied, irrespective of the wash/no wash treatment. The amplitude of the signal decreased significantly after washing (cf. Figs. 5 and 7), suggesting that most PN molecules were on the skin surface and were removed by washing. We observed the same lifetime when TMPyP, a PS that penetrates the skin and locates in the stratum corneum [41], was used instead of PN. Washing in this case reduced the signal's amplitude only by 30%, which confirms the good penetration ability of TMPyP.

The lifetime of 18 ± 2 μs is longer than that reported by Baier *et al.* [28] in a similar *ex vivo* porcine skin model (8 ± 2 μs), however, these authors excited endogenous PSs sitting probably in deeper skin layers, whereas our exogenouslyapplied PSs are in the stratum corneum. The difference in lifetime thus most likely reflects the different microenvironment of $^1O_2$ in both experiments [37].

In the presence of 0.05% LC-6 or 0.1% α-tocopherol and for washed skin samples, the $^1O_2$ lifetime was clearly shorter and almost indistinguishable (5 ± 2 and 3 ± 2 μs, respectively using PN as PS) indicating that both antioxidants quench $^1O_2$ to a similar extent in the skin (Fig. 7). Interestingly, when the skin was not washed after application of the cream a second, longer-lived component (13 μs) was observed in the case of LC-6 but not in the case of α-tocopherol. One possible explanation is that LC-6 is more able to penetrate into the stratum corneum and is therefore less available for quenching $^1O_2$ molecules on the surface. As the goal of the article was to study processes in the skin, we made no further efforts to ascertain this hypothesis. As a final test, we added 300 μL of a 0.1 mM LC-6 solution in DMSO to the skin sample containing TMPyP and were rewarded with a $^1O_2$ lifetime decrease from 18 ± 2 to 8 ± 3 μs (Fig. 8), confirming the LC-6 ability to quench $^1O_2$ in the stratum corneum.

In conclusion, we have found that LC-6 is a potent $^1O_2$ scavenger, capable of deactivating this reactive oxygen species with a rate

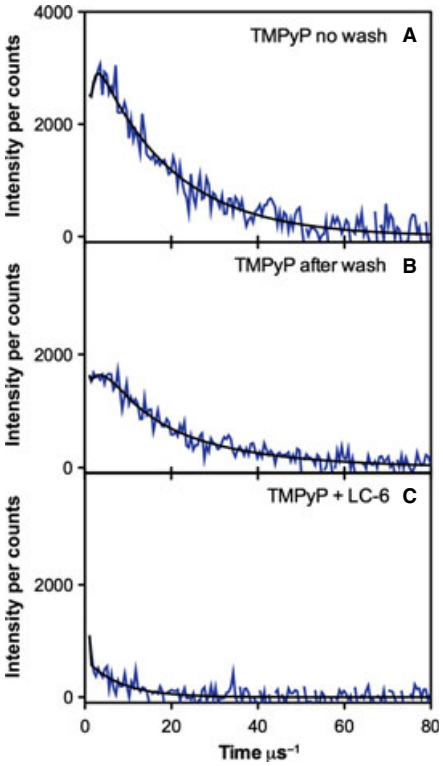

Figure 8 Time-resolved luminescence decays recorded on 532 nm excitation of *ex vivo* porcine skin treated with the water-soluble TMPyP. (A) TMPyP treated skin before wash. Fitted parameters: $\tau_T = 1 \pm 0.6$ μs; $\tau_\Delta = 18 \pm 2$ μs. (B) TMPyP treated skin after wash. Fitted parameters: $\tau_T = 1.5 \pm 0.6$ μs; $\tau_\Delta = 17 \pm 3$ μs. (C) TMPyP treated skin after apply 0.1 mM LC-6 in DMSO. Fitted parameters: $\tau_\Delta = 8 \pm 3$ μs.

constant of $(1.3 \pm 0.1) \times 10^8$ M^{-1} s^{-1}. The anti-singlet oxygen activity of LC-6 has also been demonstrated in *ex vivo* porcine skin samples.

Acknowledgments

This work has been supported by the Spanish Ministry of Economy and Competitiveness (grant No. CTQ2010-20870-C03-01) and by Lipotec S.A. M.G-D. thanks the Comissionat per Universitats i Recerca del Departament d'Innovació, Universitats I Empresa de la Generalitat de Catalunya i del Fons Social Europeu for a predoctoral fellowship.

References

1. Bogdan Allemann, I. and Baumann, L. Antioxidants used in skin care formulations. *Skin Therapy Lett.* **13**, 5–7 (2008).
2. Dreher, F. and Maibach, H. Protective effects of topical antioxidants in humans. *Curr. Probl. Dermatol.* **29**, 157–164 (2001).
3. Emerit, I. Free radicals and aging of the skin. *EXS.* **62**, 328–341 (1992).
4. Cebrian, J., Messeguer, A., Facino, R.M. and Garcia Anton, J.M. New anti-RNS and -RCS products for cosmetic treatment. *Int. J. Cosmet. Sci.* **27**, 271–278 (2005).
5. Manda, G., Nechiflor, M.T. and Neagu, T. Reactive oxygen species, cancer and anticancer therapies. *Current Chem. Biol.* **3**, 22–46 (2009).
6. Davies, K.J. An overview of oxidative stress. *IUBMB Life* **50**, 241–244 (2000).
7. Cross, C.E., van der Vliet, A., Louie, S., Thiele, J.J. and Haliwell, B. Oxidative stress and antioxidants at biosurfaces: plants, skin, and respiratory tract surfaces. *Environ. Health Perspect.* **106**, 1241–1251 (1998).
8. Ziech, D., Franco, R., Pappa, A. and Panayiotidis, M.I. Reactive oxygen species (ROS)–induced genetic and epigenetic alterations in human carcinogenesis. *Mutat. Res.* **711**, 167–173 (2011).
9. Fisher, G.J., Kang, S., Varani, J., Bata-Csorgo, Z., Wan, Y., Datta, S. and Voorhees, J.J. Mechanisms of photoaging and chronological skin aging. *Arch. Dermatol.* **138**, 1462–1470 (2002).
10. Krutmann, J. Ultraviolet A radiation-induced biological effects in human skin: relevance for photoaging and photodermatosis. *J. Dermatol. Sci.* **23**, S22–S26 (2000).
11. Regensburger, J., Knak, A., Maisch, T., Landthaler, M. and Baumler, W. Fatty acids and vitamins generate singlet oxygen under UVB irradiation. *Exp. Dermatol.* **21**, 135–139 (2012).
12. Baumler, W., Regensburger, J., Knak, A., Felgentrager, A. and Maisch, T. UVA and endogenous photosensitizers–the detection of singlet oxygen by its luminescence. *Photochem. Photobiol. Sci.* **11**, 107–117 (2012).
13. Dalle Carbonare, M. and Pathak, M.A. Skin photosensitizing agents and the role of reactive oxygen species in photoaging. *J. Photochem. Photobiol. B: Biol.*, **14**, 105–124 (1992).
14. Baier, J., Maisch, T., Maier, M., Engel, E., Landthaler, M. and Baumler, W. Singlet oxygen generation by UVA light exposure of endogenous photosensitizers. *Biophys. J .* **91**, 1452–1459 (2006).
15. Dwivedi, A., Mujtaba, S.F., Kushwaha, H.N., Ali, D., Yadav, N., Singh, S.K. and Ray, R.S. Photosensitizing mechanism and identification of levofloxacin photoproducts at ambient UV radiation. *Photochem. Photobiol.* **88**, 344–355 (2012).
16. Vargas, F., Zoltan, T., Ramirez, A.H. *et al.* Studies of the photooxidant properties of antibacterial fluoroquinolones and their naphthalene derivatives. *Pharmazie.* **64**, 116–122 (2009).
17. Moore, D.E. Drug-induced cutaneous photosensitivity: incidence, mechanism, prevention and management. *DrugSaf.* **25**, 345–372 (2002).
18. Viola, G., Miolo, G., Vedaldi, D. and Dall'Acqua, F. In vitro studies of the phototoxic potential of the antidepressant drugs amitriptyline and imipramine. *Farmaco* **55**, 211–218 (2000).
19. Regensburger, J., Lehner, K., Maisch, T. *et al.* Tattoo inks contain polycyclic aromatic hydrocarbons that additionally generate deleterious singlet oxygen. *Exp.Dermatol.* **19**, e215–e281 (2010).
20. Buenger, J., Ackermann, H., Jentzsch, A. *et al.* An interlaboratory comparison of methods used to assess antioxidant potentials. *Int. J. Cosmet. Sci.* **28**, 135–146 (2006).
21. Montoliu, C., Llansola, M., Saez, R., Yenes, S., Messeguer, A. and Felipo, V. Prevention of glutamate neurotoxicity in cultured neurons by 3,4-dihydro-6-hydroxy-7-methoxy-2,2-dimethyl-1(2H)-benzopyran (CR-6), a scavenger of nitric oxide. *Biochem.Pharmacol.* **58**, 255–261 (1999).
22. Irurre Jr, J., Casas, J., Ramos, I. and Messeguer, A. Inhibition of rat liver microsomal lipid peroxidation elicited by 2,2-dimethylchromenes and chromans containing fluorinated moieties resistant to cytochrome P-450 metabolism. *Bioorg. Med. Chem.* **1**, 219–225 (1993).
23. Yenes, S., Commandeur, J.N., Vermeulen, N.P. and Messeguer, A. In vitro biotransformation of 3,4-dihydro-6-hydroxy-2,2-dimethyl-7-methoxy-1(2H)-benzopyran (CR-6), a potent lipid peroxidation inhibitor and nitric oxide scavenger, in rat liver microsomes. *Chem. Res.Toxicol.* **17**, 904–913 (2004).
24. Miranda, M., Muriach, M., Almansa, I. *et al.* CR-6 protects glutathione peroxidase activity in experimental diabetes. *Free Radic. Biol. Med* **43**, 1494–1498 (2007).
25. Sanvicens, N., Gomez-Vicente, V., Messeguer, A. and Cotter, T.G. The radical scavenger CR-6 protects SH-SY5Y neuroblastoma cells from oxidative stress-induced apoptosis: effect on survival pathways. *J. Neurochem.* **98**, 735–747 (2006).
26. Sanvicens, N., Gomez-Vicente, V., Masip, I., Messeguer, A. and Cotter, T.G. Oxidative stress-induced apoptosis in retinal photoreceptor cells is mediated by calpains and caspases and blocked by the oxygen radical scavenger CR-6. *J. Biol. Chem.* **279**, 39268–39278 (2004).
27. Ohara, K., Origuchi, T., Kawanishi, K. and Nagaoka, S. Behavior of singlet oxygen in vitamin E emulsion. *Bull. Chem. Soc. Jpn.* **81**, 345–347 (2008).
28. Baier, J., Maisch, T., Maier, M., Landthaler, M. and Baumler, W. Direct detection of singlet oxygen generated by UVA irradiation in human cells and skin. *J. Invest. Dermatol.* **127**, 1498–1506 (2007).
29. Davies, M.J. Reactive species formed on proteins exposed to singlet oxygen. *Photochem. Photobiol. Sci.* **3**, 17–25 (2004).
30. Redmond, R.W. and Kochevar, I.E. Spatially resolved cellular responses to singlet oxygen. *Photochem. Photobiol.* **82**, 1178–1186 (2006).
31. Piette, J. Biological consequences associated with DNA oxidation mediated by singlet oxygen. *J.Photochem.Photobiol. B: Biol* **11**, 241–260 (1991).
32. Nonell, S. and Braslavsky, S.E.. Time-resolved singlet oxygen detection. In *Singlet Oxygen, UV-A and Ozone* (L. Packer, H.Sies., Eds.). *Methods Enzymol.*. **319**, 37–49 (2000).
33. Jimenez-Banzo, A., Ragas, X., Kapusta, P. and Nonell, S. Time-resolved methods in biophysics. 7. Photon counting vs. analog time-

resolved singlet oxygen phosphorescence detection. *Photochem. Photobiol. Sci.* **7**, 1003–1010 (2008).
34. Kalia, Y.N., Alberti, I., Sekkat, N., Curdy, C., Naik, A. and Guy, R.H. Normalization of stratum corneum barrier function and transepidermal water loss *in vivo*. *Pharm. Res.* **17**, 1148–1150 (2000).
35. Sintov, A.C., Krymberk, I., Daniel, D., Hannan, T., Sohn, Z. and Levin, G. Radiofrequency-driven skin microchanneling as a new way for electrically assisted transdermal delivery of hydrophilic drugs. *J. Control. Release* **89**, 311–320 (2003).
36. Caucanas, M., Montastier, C., Pierard, G.E. and Quatresooz, P. Dynamics of skin barrier repair following preconditioning by a biotechnology-driven extract from samphire (Crithmum maritimum) stem cells. *J. Cosmet. Dermatol.* **10**, 288–293 (2011).
37. Wilkinson, F., Phillip Helman, W. and Ross, A.B. Rate constants for the decay and reactions of the lowest electronically excited singlet state of molecular oxygen in solution. An expanded and revised compilation. *J. Phys. Chem. Ref. Data* **24**, 663–677 (1995).
38. Oliveros, E., Suardi-Murasecco, P., Aminian-Saghafi, T., Braun, A.M. and Hansen, H.J. 1H-Phenalen-1-one: photophysical properties and singlet-oxygen production. *Helv. Chim. Acta* **74**, 79–90 (1991).
39. Schmidt, R., Tanielian, C., Dunsbach, R. and Wolff, C. Phenalenone, a universal reference compound for the determination of quantum yields of singlet oxygen O2(1Δg) sensitization. *J.Photochem.Photobiol.A:Chem*, **79**, 11–17 (1994).
40. Flors, C. and Nonell, S. On the phosphorescence of 1H-phenalen-1-one. *Helv.Chim. Acta.* **84**, 2533–2539 (2001).
41. Eichner, A., Pereira Gonzales, F., Felgenträger, A. *et al.* Dirty hands: photodynamic killing of human pathogens like EHEC, MRSA. *Photochem. Photobiol. Sci.* **12**, 135–147 (2013).
42. Kobayashi, K., Maehata, Y., Kawamura, Y. *et al.* Direct assessments of the antioxidant effects of the novel collagen peptide on reactive oxygen species using electron spin resonance spectroscopy. *J.Pharmacol.Sci* **116**, 97–106 (2011).
43. Yoshida, A., Yoshino, F., Tsubata, M., Ikeguchi, M., Nakamura, T. and Lee, M.C. Direct assessment by electron spin resonance spectroscopy of the antioxidant effects of French maritime pine bark extract in the maxillofacial region of hairless mice. *J. Clin. Biochem. Nutr* **49**, 79–86 (2011).
44. Iannone, A., Rota, C., Bergamini, S., Tomasi, A. and Canfield, L.M. Antioxidant activity of carotenoids: an electron-spin resonance study on beta-carotene and lutein interaction with free radicals generated in a chemical system. *J. Biochem. Mol. Toxicol.* **12**, 299–304 (1998).
45. Ozawa, T., Hanaki, A. and Matsuo, M. Reactions of superoxide ion with tocopherol and its model compounds: correlation between the physiological activities of tocopherols and the concentration of chromanoxyl-type radicals. *Biochem. Int.* **6**, 685–692 (1983).
46. Osawa, A., Ishii, Y., Sasamura, N., Morita, M., Kasai, H., Maoka, T. and Shindo, K. Characterization and antioxidative activities of rare C (50) carotenoids-sarcinaxanthin, sarcinaxanthin monoglucoside, and sarcinaxanthin diglucoside-obtained from Micrococcus yunnanensis. *J. Oleo.Sci.* **59**, 653–659 (2010).
47. Pastore, D., Laus, M.N., Tozzi, D., Fogliano, V., Soccio, M. and Flagella, Z. New tool to evaluate a comprehensive antioxidant activity in food extracts: bleaching of 4-nitroso-N,N-dimethylaniline catalyzed by soybean lipoxygenase-1. *J. Agric. Food Chem.* **57**, 9682–9692 (2009).
48. Baghiani, A., Charef, N., Djarmouni, M., Saadeh, H.A., Arrar, L. and Mubarak, M.S. Free radical scanvenging and antioxidant effects of some anthraquinone derivatives. *Med. Chem.* **7**, 639–644 (2011).
49. Niki, E. Assessment of antioxidant capacity *in vitro* and *in vivo*. *Free Radic. Biol. Med.* **49**, 503–515 (2010).
50. Cao, G., Alessio, H.M. and Cutler, R.G. Oxygen-radical absorbance capacity assay for antioxidants. *Free Radic. Biol. Med.* **14**, 303–311 (1993).
51. Aizawa, K., Iwasaki, Y., Ouchi, A., Inakuma, T., Nagaoka, S., Terao, J. and Mukai, K. Development of singlet oxygen absorption capacity (SOAC) assay method. 2. Measurements of the SOAC values for carotenoids and food extracts. *J. Agric. Food Chem.* **59**, 3717–3729 (2011).
52. Ouchi, A., Aizawa, K., Iwasaki, Y., Inakuma, T., Terao, J., Nagaoka, S. and Mukai, K. Kinetic study of the quenching reaction of singlet oxygen by carotenoids and food extracts in solution. Development of a singlet oxygen absorption capacity (SOAC) assay method. *J. Agric. Food Chem.* **58**, 9967–9978 (2010).
53. Hideg, E. Detection of free radicals and reactive oxygen species. *Methods Mol. Biol.* **274**, 249–260 (2004).
54. Kim, J.I., Lee, J.H., Choi, D.S., Won, B.M., Jung, M.Y. and Park, J. Kinetic study of the quenching reaction of singlet oxygen by common synthetic antioxidants (tert-butylhydroxyanisol, tert-di-butylhydroxytoluene, and tert-butylhydroquinone) as compared with alpha-tocopherol. *J. Food Sci.* **74**, C362–C369 (2009).
55. Gruszka, J., Pawlak, A. and Kruk, J. Tocochromanols, plastoquinol, and other biological prenyllipids as singlet oxygen quenchers-determination of singlet oxygen quenching rate constants and oxidations products. *Free Radic. Biol. Med.* **45**, 920–928 (2008).
56. Grams, G.W. and Eskins, K. Dye-sensitized photooxidation of tocopherols. Correlation between singlet oxygen reactivity and vitamin E activity. *Biochemistry* **11**, 606–608 (1972).
57. Kanofsky, J.R. Measurement of Singlet-Oxygen *In Vivo*: progress and Pitfalls. *Photochem. Photobiol.* **87**, 14–17 (2011).